

Document downloaded from:

<http://hdl.handle.net/10251/57921>

This paper must be cited as:

Padin Devesa, J.; Martín Furones, ÁE.; Anquela Julián, AB. (2012). ARCHAEOLOGICAL MICROGRAVIMETRIC PROSPECTION INSIDE DON CHURCH (VALENCIA, SPAIN). *Journal of Archaeological Science*. 39(2):547-554. doi:10.1016/j.jas.2011.10.012.



The final publication is available at

<http://dx.doi.org/10.1016/j.jas.2011.10.012>

Copyright Elsevier

Additional Information

Document downloaded from:

<http://hdl.handle.net/10251/57921>

This paper must be cited as:

Padin Devesa, J.; Martín Furones, ÁE.; Anquela Julián, AB. (2012). ARCHAEOLOGICAL MICROGRAVIMETRIC PROSPECTION INSIDE DON CHURCH (VALENCIA, SPAIN). *Journal of Archaeological Science*. 39(2):547-554. doi:10.1016/j.jas.2011.10.012.



The final publication is available at

<http://dx.doi.org/10.1016/j.jas.2011.10.012>

Copyright Elsevier

Additional Information

1
2
3
4
5
6
7
8
9
10
11
12
13
14
15
16
17
18
19
20
21
22
23
24
25
26
27
28
29
30
31
32
33
34
35
36
37
38
39
40
41
42
43
44
45
46
47
48
49
50
51
52
53
54
55
56
57
58
59
60
61
62
63
64
65

ARCHAEOLOGICAL MICROGRAVIMETRIC PROSPECTION INSIDE DON CHURCH (VALENCIA, SPAIN)

Jorge Padín, Angel Martín*, Ana Belén Anquela

Department of Cartographic Engineering, Geodesy and Photogrammetry, Polytechnic
University of Valencia, C\Camino de Vera s/n, Valencia 46022, Spain.

* Corresponding author. Tel +(34) 96-3877007.

E-mail adress: aemartin@upvnet.upv.es

Abstract

The microgravimetric surveying technique is applicable to the detection of shallow subsurface structures if a lateral density contrast is presented, and thus, it is a valid technique for archaeological prospection. In this paper, this technique has been revealed to be an efficient tool for archaeological studies, such as those performed inside Don Church (18th century), located in the urban area of Alfafar town, Valencia (Spain), where a buried crypt, suggested by different boreholes drilled during the second restoration process in 1993, is expected. Details of the site's characteristics, topographic survey procedures, microgravimetric field operations, data collection and gravity reduction operations (where the inner building effect of walls, pillars and the altar is confirmed as one of the most important) are also presented. Finally, the results confirm the buried crypt.

1
2
3
4
5
6
7
8
9
10
11
12
13
14
15
16
17
18
19
20
21
22
23
24
25
26
27
28
29
30
31
32
33
34
35
36
37
38
39
40
41
42
43
44
45
46
47
48
49
50
51
52
53
54
55
56
57
58
59
60
61
62
63
64
65

Keywords: Microgravimetric survey; archaeological prospection; Don Church;
Valencia.

1 Introduction

Gravity and microgravimetric studies have been widely and routinely used in geophysics, geodesy, geodynamics, geology, mineral and oil exploration and engineering applications (Burger, 1992; Sharma, 1997; Torge, 1989). Likewise, bibliographic references regarding the application of the microgravimetric technique in archaeological prospection are numerous; for example, microgravimetric and gravity gradient techniques are applied in Butler (1984) for the detection of subsurface cavities and tunnels; Friedrich et al. (1996) used microgravimetry to detect hidden cavities and cisterns in the Hagia Sophia's subsurface structure, confirming the accuracy and efficiency of this technique to investigate subsurface structures of historical buildings; Ranieri and Sambuelli (1996) evaluated the use of microgravity measurements to characterise density anomalies in surrounding tunnels; Yule et al. (1998) conducted a microgravimetric investigation to detect subsurface cavities or other anomalous conditions that could threaten the stability of switchyard structures; Beres et al. (2001), Styles et al. (2005) and Leucci and De Giorgi (2010) used microgravimetric surveys to map subsurface karstic features; Ebrahimzadeh (2004) used microgravity measurements to detect subsurface cavities or other anomalous conditions that threaten the stability of the foundation in the technical University of Tehran; Rodríguez et al. (2007) conducted a microgravimetric study in the Vall de Crist Carthusian Monastery (Castellón, Spain) to detect and map a shallow subsurface rainwater cistern, proving that the microgravimetric technique is an efficient tool for cultural heritage restoration studies;

1 and finally, the microgravimetric technique has proven useful in urban areas to map
2 well-defined structures, such as doline filled with urban debris (Mochales et al., 2008).
3
4
5
6

7 In this paper, we report a microgravimetric prospection study for archaeological
8 purposes inside a historical building. The first part of the paper is devoted to the
9 theoretical methodology and practical considerations to reduce, correct and process the
10 microgravimetric observations. The second part presents the church and the
11 microgravimetric maps related to the reductions, corrections and processing of the
12 observations, which are followed by the final map of the local residual Bouguer
13 anomalies. A microgravimetric inversion of a cross-section and analysis and discussion
14 of the results ends this section. The paper ends with some conclusions about the utility
15 of the technique, including practical considerations for a good microgravimetric survey
16 and the archaeological benefits obtained in the Don Church prospection.
17
18
19
20
21
22
23
24
25
26
27
28
29
30
31

32 Therefore, this paper can be considered as a case study of microgravimetric technique
33 applied to archaeological prospection. All the reductions and corrections to the
34 gravimetric observations are applied (most of the references before did not include the
35 complete sequence but only some of them), where we highlight the inner building effect
36 as one of the most important in the reduction process when the propection is located
37 inside a building.
38
39
40
41
42
43
44
45
46
47
48
49
50
51
52
53
54
55
56
57
58
59
60
61
62
63
64
65

2 Methodology

2.1 Survey details and field procedures

Data were collected with the Lacoste & Romberg D203 gravity meter. This gravity meter has electronic levels and is equipped with an electrostatic feedback system. The nominal sensitivity is approximately 1 μGal ($1 \mu\text{Gal} = 1.10^{-8} \text{ms}^{-2}$); however, its use in field conditions introduces accidental errors in the observations that should be appropriately minimised to achieve relative observations with an accuracy of 5-7 μGal . A list of error sources, their standard deviations and additional precautions to be adopted to minimise their impact can be found in Torge (1989) and Qianshen et al. (1996). These additional precautions include orientation of the instrument with respect to the magnetic field, the readings can only be taken 5 minutes after releasing the clamp, at least three readings should be performed for each station using only the feedback system, and hand carrying was employed during the survey to avoid vibration shock and to ensure careful operation.

In the case study presented, the gravity station grid was marked on the floor with chalk, and the nodes were used for gravity observations. The rules used for the station spacing and field operations with the Lacoste & Romberg are described in Qianshen et al. (1996).

A total-station surveying instrument was used to determine the horizontal and vertical positions of the station points in a local reference frame with an error better than 0.02 m.

Microgravimetric surveys require effective and accurate consideration of the effects

1 given by infrastructures, such as buildings (including which the microgravimetric
2 survey is performed), as well as those given by topography near a gravity station. A
3
4 local survey with the same total-station was performed for the sake of terrain and
5
6 building corrections.
7
8
9

10 11 **2.2 Gravity corrections and reductions**

12
13
14
15
16
17 Corrections to microgravimetric observations are needed to compensate gravity
18
19 variations due to natural causes (earth tides or atmospheric variations), instrumental
20
21 causes (drift), observational causes (instrumental height) or geographical situation
22
23 causes (variations in latitude or corrections for terrain and buildings). In the following,
24
25 these corrections are presented in the same order as they are applied to the raw
26
27 microgravimetric data. They are well known since many decades and are applied in a
28
29 standard way, so a short description is only need.
30
31
32
33
34
35

36 **2.2.1 Tidal effects and correction**

37
38
39
40
41 To predict the tide component, version 3.32 of Professor Wenzel's ETERNA software
42
43 package with Hartmann-Wenzel Earth tide catalogue was used (Wenzel, 1999).
44
45
46 Parameters for amplitude and phase-difference for the principal tidal waves were fixed
47
48 to zero and 1.164, respectively (Boedecker, 1988).
49
50
51
52
53
54
55
56
57
58
59
60
61
62
63
64
65

2.2.2 Instrumental height correction

For the purpose of reducing the gravimetric reading to the ground mark, the theoretical free-air gradient of 308.6 μGal by one meter was used, and the height of the instrument above the station level was carefully measured (Torge, 1989).

2.2.3 Atmospheric pressure correction

This reduction has to be applied to account for the difference between the actual atmospheric pressure and the normal atmospheric pressure at the station (Boedecker and Ritcher, 1981). International Association of Geodesy (IAG) resolution No 9, recommends the use of the following formulae for atmospheric gravity reduction (Torge, 1989):

$$dg_p = 0.30(P_i - P_{in}) \quad \mu\text{Gal}$$
$$P_{in} = 1013.25 \left(1 - \frac{0.0065 H}{288.15} \right)^{5.2559} \quad (1)$$

where H is the orthometric height of the station, P_i is the measured value of the pressure at the station and P_{in} is the normal pressure (both in hPa).

2.2.4 Instrumental drift and drift correction

The drift of the Lacoste & Romberg D203 gravity meter can be considered linear for short periods of time (6-8 hours), (Martín et al., 2011) and it is corrected applying this linear behaviour to the rest of the readings based on repeated measurements at base stations.

2.2.5 Latitude correction (normal gravity correction)

The rotation of the Earth and its nonspherical shape produce an increase in gravity values with latitude that can be taken into account by subtracting the normal ellipsoidal gravity to the observations, or, for the relatively small areas of microgravity surveys, it is sufficient to assign a reference latitude to the base station and to use the following expression to take into account the augmentation of gravity on the North direction (Qianshen et al., 1996):

$$dg_p = \pm 0.81 \sin 2\psi \Delta L \quad \mu Gal \quad (2)$$

where ΔL is the distance to the North or South direction to the base station in meters, and ψ is the reference latitude (latitude of the base station). This correction is positive if the station is located south of the base station; otherwise, it is negative.

2.2.6 Free-air and Bouguer correction

The free-air and Bouguer corrections are computed through the following equation (Ebrahimzadeh, 2004; Torge, 1989; Yule et al., 1997):

$$dg_{F+B} = \pm(308.6 - 41.91\rho)\Delta h \quad \mu Gal \quad (3)$$

where ρ is the average density of the materials and Δh is the difference in metres between the elevation of the measurement station and the elevation of the reference level. The sign of this equation is positive if the reference level is under the measurement level and negative if it is higher.

2.2.7 Terrain correction

Bouguer correction is completed with the terrain correction (Torge, 1989). The expression of Nagy (Nagy, 1966), based on the attraction generated by a rectangular prism, is used to compute this correction:

$$dg_t = G\rho \left[-x \ln(y+r) - y \ln(x+r) + z \arctan\left(\frac{xy}{zr}\right) \right]_{x_1}^{x_2} \left[y_1 \right]_{y_1}^{y_2} \left[z_1 \right]_{z_1}^{z_2} \quad (4)$$

where G is the gravitational constant, ρ is the mean density of the topography and

$r = \sqrt{x^2 + y^2 + z^2}$, where the coordinate system is a local one centred on the

observation point, so that it changes for every microgravimetric station.

2.2.8 Correction for building effects

In microgravimetry, particular caution should be taken in correcting for buildings, as their effect can be greater than the amplitude of the expected anomalies (Debeglia and Dupont, 2002, Qianshen et al., 1996). Most buildings have a regular geometrical shape or various compositions of certain regular geometric elements (e.g., cylinder, sphere, rectangle), and thus, the computation of the attraction they exert can be performed using equation 4. The precision of this correction depends on the accuracy of the digital model of the elements of these buildings and on the correct adoption of the mean density value for walls, pillars, floors or roofs. An alternative procedure to computing an estimation of the mean density for the building corrections and mean values for that densities can be found in Qianshen et al. (1996), page 63.

In our case, the most important building to take into account is the one for which the survey is being conducted (it can be named the inner building). One important aspect to take into account is that the inner building effect could be extremely high for points situated very near the element (2 metres or less), where the gradient introduced by the element (a wall for example) is difficult to estimate and can introduce a significant distorsion effect in the gravity observation. This effect can be seen in Fig. 1, where the influence of a rectangular building with 1 metre wide walls with a 2.1 gr/cm^3 density and a height of 10 metres is modelled, suggesting that observations near the walls should not be done.

FIGURE 1

2.3 Data processing

When all the corrections and reductions explained in section 2.2 have been applied to the microgravimetric observations, the final Bouguer gravities are obtained, g_B . Subtracting the Bouguer gravity obtained at the base station, g_{base} , from the Bouguer gravities at each station by

$$\Delta g_B = g_B - g_{base} \quad (5)$$

results in the final residual Bouguer gravity anomaly. In the same way, the term “residual” can be applied to the gravity observations (that is ‘residual gravity observations’) if they are formed by subtracting the gravity observation at the base station to the gravity observations at each station.

After the computation of the final residual Bouguer gravity anomalies, separation between local and regional gravimetric components is needed to differentiate between anomalies from local, near surface masses (which are of interest in this kind of studies) and those arising from larger and deeper structures (Dobrin and Savit, 1988; Torge, 1989; Sharma, 1997). Due to the small dimensions of the studied areas in archaeological research, the adjustment of a low degree polynomial to the final residual Bouguer gravity anomaly is recommended, so it is assumed that a polynomial surface adequately models the field’s regional component (see for instance, Camacho et al., 1994; Montesinos et al., 1999).

1 If the microgravity observation is performed in the nodes of a grid, the contour maps
2 can be created directly without any interpolation technique consideration or error, but if
3
4 the nodes do not conform to a regular grid an interpolation is needed. A geostatistical
5
6 method such as kriging is highly recommended.
7
8
9

10
11 Finally, these contour maps are the basis of the analysis, discussion and conclusions.
12
13
14
15

16 **3 A Case study: Don Church (Alfajar, Valencia)**

17
18
19
20

21 Don Church is located in the urban area of Alfajar town, Valencia (eastern part of
22
23 Spain). The geological characteristics inside this town are quite homogeneous and can
24
25 be described as the result of a terrain hollow depression formed in the Miocene era,
26
27 which was subsequently filled by alluvial deposits. This process generates horizontal
28
29 layers of marls and clay alternating with gravels and sands.
30
31
32
33
34
35

36 The actual church was constructed between 1736 and 1748. The church was restored in
37
38 1918 and 1993. During the second restoration, the existence of a gothic floor under the
39
40 present floor was suggested, indicating that the actual church was constructed above
41
42 another one, so various boreholes were drilled, Fig 2. One of these boreholes (B3 in Fig.
43
44 2) showed part of an old wall identified as gothic style. Another one (B1 in Fig. 2)
45
46 found parts of the ceiling of a buried crypt situated at, approximately, 1 m under the
47
48 actual floor. This crypt, apparently, longitudinally crossed the church. Thus, the main
49
50 objective of the microgravimetric prospection is this crypt.
51
52
53
54
55
56
57
58
59
60
61
62
63
64
65

1 The situation of the profiles and the ground plan of the church can be seen in Fig. 2. The
2 8 profiles are situated at least 2 metres away from the walls. The observed points in
3 these profiles are separated by 1 metre in the central area, where the crypt was expected,
4 and 2 metres out of this area. Finally Fifty-one points have been observed (including the
5 base station). A precise topographic survey of the terrain (Fig. 3), the nearby buildings
6 (Fig. 4), and the structures of the church (black elements in Fig. 2), was performed.
7
8
9
10
11
12
13
14
15
16

17 Fig. 5 shows the plot of the observed residual gravity anomalies correcting the
18 observations only for tide, instrumental height, atmospheric and drift effects, where the
19 situation of the altar (0.6 metre above the floor) is clearly drawn. The statistical resume
20 of these values can also be found in table 1.
21
22
23
24
25
26
27
28

29 A density value of 2.1 gr/cm^3 is introduced for Bouguer and terrain correction. This
30 value is the mean density for marls, clay, gravels and sands (Telford et al., 1990), that is
31 the mean density of the geological materials located in the survey area.
32
33
34
35
36
37
38

39 After latitude, free-air, Bouguer, terrain and near-buildings corrections (Fig. 6), the
40 situation of the altar is blurred, and the geometry of the prospection presents higher
41 gravity anomaly values in the centre of the church than in the periferic areas. This
42 geometry is caused by the construction elements of the church (walls and pillars). Fig. 7
43 presents the correction of these near elements, showing the typical cross-configuration
44 of a church (it can be compared with Fig. 2). The gravimetric effect of the structure of
45 the altar is separated, Fig. 8, because the density of this structure is low to that
46 considered in the Bouguer correction (the altar is constructed by the introduction of
47 compacted debris material over the original terrain, not over the original terrain
48
49
50
51
52
53
54
55
56
57
58
59
60
61
62
63
64
65

1 directly), so an excess in density is introduced in the Bouguer correction and should be
2 eliminated. Finally, Fig. 9 presents the final residual Bouguer anomalies corrected by
3 the effect of all these near elements. In table 1 the statistical resume of residual Bouguer
4 anomalies and residual Bouguer anomalies after correction for these structural features
5 can be found. The standard deviation is reduced from 58 to 13-15 μGal compared with
6 the residual gravity anomalies corrected only for tide, instrumental height, atmospheric
7 and drift effects and the range of the values have been reduced from 186 to 55-60 μGal .
8 These results confirm that the reduction process eliminates the major part of the
9 gravimetric signal and only the interested part, located in the floor of the church, is
10 retained.
11
12
13
14
15
16
17
18
19
20
21
22
23
24
25
26

27 Given the dimensions of the working area and taking into consideration the low gradient
28 of the final residual Bouguer anomalies (Fig. 9), it seems logical to use a one-degree
29 polynomial (that is, a plane) for local-regional gravimetric field separation. The adjusted
30 polynomial surface can be seen in Fig. 10, and the result obtained after the subtraction
31 of this polynomial surface to the final residual Bouguer anomalies, that is, the final local
32 residual Bouguer anomalies, can be seen in Fig. 11. The last column of table 1 give the
33 statistical resume. The statistical behaviour is similar to the column corresponding to the
34 final residual Bouguer anomalies.
35
36
37
38
39
40
41
42
43
44
45
46
47
48

49 In figure 11, the footprint of the expected longitudinal crypt, corresponding to a low
50 longitudinal gravity anomaly values can be seen. Low longitudinal gravity anomaly
51 value can be seen in the entrance of the church, the same low gravity anomaly is located
52 in the altar but without the longitudinal trend. The low gravity anomalies disappears in
53 the centre of the church, most likely due to a full up process with debris material in this
54
55
56
57
58
59
60
61
62
63
64
65

1 part of the crypt in the construction process of the actual church, or simply because the
2 crypt did not cross all the church in a longitudinal way: it ends 6-7 meters away the
3
4 entrance and the low gravity anomalies located in the altar could be still influenced by
5
6 the presence of the altar.
7
8
9

10
11
12 FIGURE 2

13
14 FIGURE 3

15
16 FIGURE 4

17
18 FIGURE 5

19
20 FIGURE 6

21
22 FIGURE 7

23
24 FIGURE 8

25
26 FIGURE 9

27
28 FIGURE 10

29
30 FIGURE 11

31
32
33
34
35
36
37
38
39 A microgravimetric inversion was performed in the AA' cross-section (Fig. 11) to fit
40
41 the expected crypt to the final local residual Bouguer anomalies. The modelling was
42
43 carried out with the GravModeler software, which performs 2D modelling of gravity
44
45 data based on the line integral approach of the classical Talwani method (Talwani et al.,
46
47 1959) using bodies of various densities embedded within a homogeneous background.
48
49
50

51
52
53 An empty (zero density value) rectangle 2.5 m wide and 1.2 m high, located 1 m under
54
55 the actual floor can explain the microgravimetric differences observed in the cross-
56
57 section (Fig. 12). Finally, this rectangle can be linked to the expected crypt.
58
59
60
61
62
63
64
65

FIGURE 10

4 Conclusions

The microgravimetric survey proved to be a valid technique for archaeological prospection due to its capacity to detect and delineate shallow structures (including surrounding ones). To obtain a clear interpretation of the Bouguer anomalies, all reductions and corrections should be applied carefully and with maximum rigour to the raw microgravimetric observations. Special emphasis should be placed on structural near elements, where the gravimetric observation must be made at a distance greater than 2 metres from the elements to avoid possible distortions in the gravimetric signal. A case study is performed in Don Church, where the expected crypt seems to be clearly found in the entrance of the church, confirming the previous suggestions based on the boreholes.

Acknowledgements

The authors would like to thank Susana De La Rubia and Blas Guijarro the opportunity to develop this prospection. The two anonymous reviewers are kindly acknowledged for their contribution with valuable comments and suggestions.

References

1
2
3
4 Beres, M., Luetscher, M., Olivier, R., 2001. Integration of ground-penetrating radar and
5 microgravimetric methods to map shallow caves. *J. Appl. Geophys.* 46, 249-262.
6

7
8
9
10
11 Boedecker, G., 1988. Absolute gravity observations, data processing standards and
12 station documentation. *Bull. Inf. Bur. Gravim. Int.* 63, 51-57.
13

14
15
16
17
18 Boedecker, G., Richter, B., 1981. The new gravity base net 1976 of the Federal
19 Republic of Germany (DSGN 76). *Bull. Geod.* 55, 250-266.
20
21

22
23
24
25
26 Burger, H.R., 1992. *Explorations geophysics of the shallow subsurface*. Prentice Hall,
27 Englewood Cliffs, London.
28

29
30
31
32
33 Butler, D.K., 1984. Microgravimetric and gravity gradient techniques for detection of
34 subsurface cavities. *Geophys.* 49(7), 1084-1096.
35
36

37
38
39
40
41 Camacho, A. G., Montesinos, F.G., Vieira, R., 1997. A three-dimensional gravity
42 inversion applied to Sao Miguel Island (Azores). *J. Geophys. Res.*, 102(B4), 7717-7730.
43
44

45
46
47
48 Debeglia, N., Dupont, F., 2002. Some critical factors for engineering and environmental
49 microgravity investigations. *J. Appl. Geophys.* 50, 435-454.
50
51

52
53
54
55 Dobrin, M.B., Savit, C H., 1988. *Introduction to geophysical prospecting*. Fourth
56 edition. McGraw-Hill, Inc.
57
58
59
60
61
62
63
64
65

1
2 Ebrahimzadeh, V., 2004. Microgravity investigations of foundation conditions. *J. Earth*
3
4 & Space Phys. 30(1), 11-14.
5
6

7
8
9 Friedrich, J., Gerstenecker, C., Gürkan, O., 1996. Gravimetric examination of Hagia
10
11 Sophia's subsurface structure. *J. Geod.* 70, 645-651.
12
13

14
15
16 Leucci, G., De Giorgi L., 2010. Microgravimetric and ground penetrating radar
17
18 geophysical methods to map the shallow karstic cavities network in a coastal area
19
20 (Marina Di Capilungo, Lecce, Italy). *Exploration Geophys.* 41, 178-188.
21
22
23

24
25
26 Martín, A., Anquela, A.B., Padín, J., Berné, J.L., 2011. On standard reductions to
27
28 relative gravity measurements. a case study through the establishment of the new local
29
30 gravity net in the province of Valencia (Spain). *Surv. Rev.* 43(319), 16-29.
31
32
33

34
35
36 Mochales, T., Casas, A.M., Pueyo, E.L., Pueyo, O., Román, M.T., Pocoví, A., Soriano,
37
38 M.A., Ansón, D., 2008. Detection of underground cavities by combining gravity,
39
40 magnetic and ground penetrating radar surveys: a case study from the Zaragoza area,
41
42 NE Spain. *Environ. Geol.* 53, 1067-1077.
43
44
45

46
47
48 Montesinos, F.G., Camacho, A.G., Vieira, R., 1999. Análisis of gravimetric anomalies
49
50 in Furnas Caldera (Sao Miguel, Azores), *J. Volcanol. and Geotherm. Res.*, 92(1-2), 67-
51
52

1 Nagy, D., 1966. The gravitational attraction of a right angular prism. *Geophys.* 31, 362-
2 371.
3

4
5
6
7 Qianshen, W., Chijun, Z., Fuzhen, J., Wenhui Z., 1996. *Microgravimetry*. Science Press,
8
9 Beijing, China.
10

11
12
13
14 Ranieri, G., Sambuelli, L., 1996. A new procedure to perform differential underground
15 gravity measurements. *J. Appl. Geophys.* 36, 123-129.
16
17
18

19
20
21 Rodríguez, I., García, F., Rodríguez, Ir. Ramírez, M., Montalvo, J.L., Benlloch, J.,
22
23 Capuz, R., 2007. Non-destructive assessment of a buried rainwater cisterna at the
24 Carthusian Monastery “Vall de Crist” (Spain, 14th century) derived by
25
26
27
28
29
30
31
32
33
34
35
36
37
38
39
40
41
42
43
44
45
46
47
48
49
50
51
52
53
54
55
56
57
58
59
60
61
62
63
64
65

microgravimetric 2D modelling. *J. cultural herit.* 8, 197-201.

Sharma, P.V., 1997. *Environmental and engineering geophysics*. Cambridge University
Press.

Styles, P., McGrath, R., Thomas, E., Cassidy, N.J., 2005. The use of microgravimetry
for cavity characterization in karstic terrains. *Q. J. Engineer. Geolog. and hydrogeolog.*
38, 155-169.

Talwani, M., Worzel, J.L., Landisman, M., 1959. Rapid gravity computations for two-
dimensional bodies with application to the Mendocino submarine fracture zone. *J.*
Geophys. Res. 64(1), 49-61.

1 Telford, W.M., Geldart, L.P., Sheriff, R.E., 1990. Applied Geophysics. 2nd edition.
2 Cambridge University Press.
3

4
5
6
7 Torge, W., 1989. Gravimetry. Ed. Walter de Gruyter.
8
9

10
11
12 Wenzel, G., 1999. Earth tide data processing package, Eterna version 3.32. User
13 manual.
14
15

16
17
18
19 Yule, D.E., Sharp, M.K., Butler, D.K., 1998. Microgravity investigations of foundation
20 conditions. Geophys. 63(1), 95-106.
21
22
23
24
25
26
27
28
29
30
31
32
33
34
35
36
37
38
39
40
41
42
43
44
45
46
47
48
49
50
51
52
53
54
55
56
57
58
59
60
61
62
63
64
65

FIGURE CAPTIONS

Fig. 1. Example of the influence of rectangular building on microgravimetric observations; for explanations see the text.

Fig. 2. Ground plan of Don Church including the profiles (P1 to P8) used for the microgravimetric observations. Black points represent the location of a borehole.

Fig. 3. Plot of the digital elevation model.

Fig. 4. Map of the near buildings modelled and corrected at the microgravimetric observations.

Fig. 5. Residual gravity anomalies (corrections for tides, instrument height, atmospheric and drift effects).

Fig. 6. Residual Bouguer anomalies (corrections for tides, instrument height, atmospheric effects, drift, latitude, free-air, Bouguer, terrain and near buildings effects).

Fig. 7. Microgravimetric correction for the near elements (walls and pillars).

Fig. 8. Microgravimetric correction for the altar.

Fig. 9. Final residual Bouguer anomalies.

Fig. 10. Adjusted polynomial surface for local-regional gravimetric field separation.

Fig. 11. Final local residual Bouguer anomalies.

Fig. 12. Microgravimetric modelled inversion of AA' cross-section.

1
2
3
4
5
6
7
8
9
10
11
12
13
14
15
16
17
18
19
20
21
22
23
24
25
26
27
28
29
30
31
32
33
34
35
36
37
38
39
40
41
42
43
44
45
46
47
48
49
50
51
52
53
54
55
56
57
58
59
60
61
62
63
64
65

Table 1. Statistical resume for different residual gravity signals. Values are presented un μGal .

| | Residual gravity observations | Residual Bouguer anomalies | Residual Bouguer anomalies after structures correction | Final local Residual Bouguer anomalies |
|----------|-------------------------------|----------------------------|--|--|
| Mean | 37.301 | 58.766 | 41.071 | 40.731 |
| σ | 58.757 | 15.717 | 13.362 | 12.626 |
| Max. | 82.856 | 84.488 | 61.159 | 62.148 |
| Min. | -103.549 | 21.872 | 6.197 | 8.464 |

Figure 1
[Click here to download high resolution image](#)

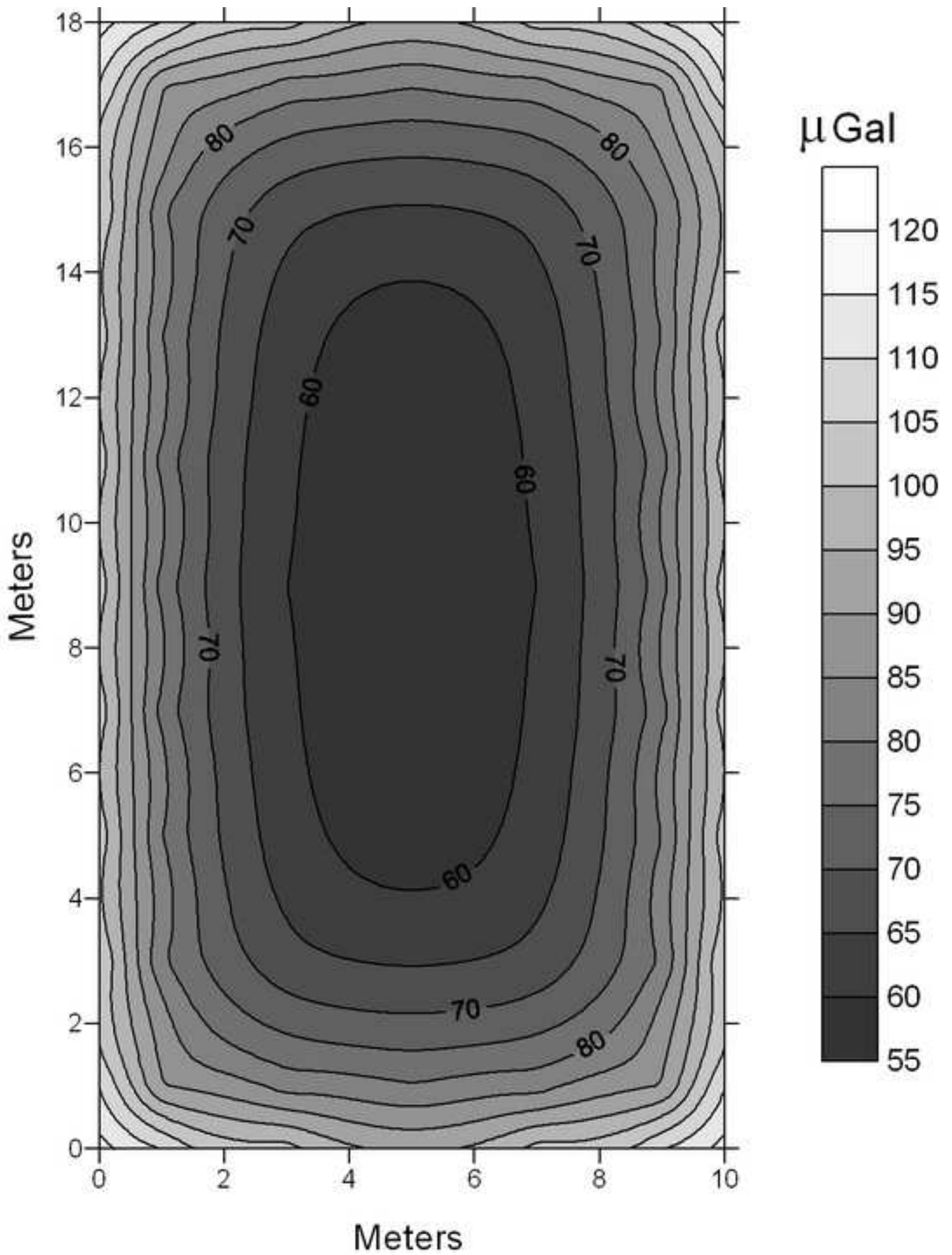


Figure 2
[Click here to download high resolution image](#)

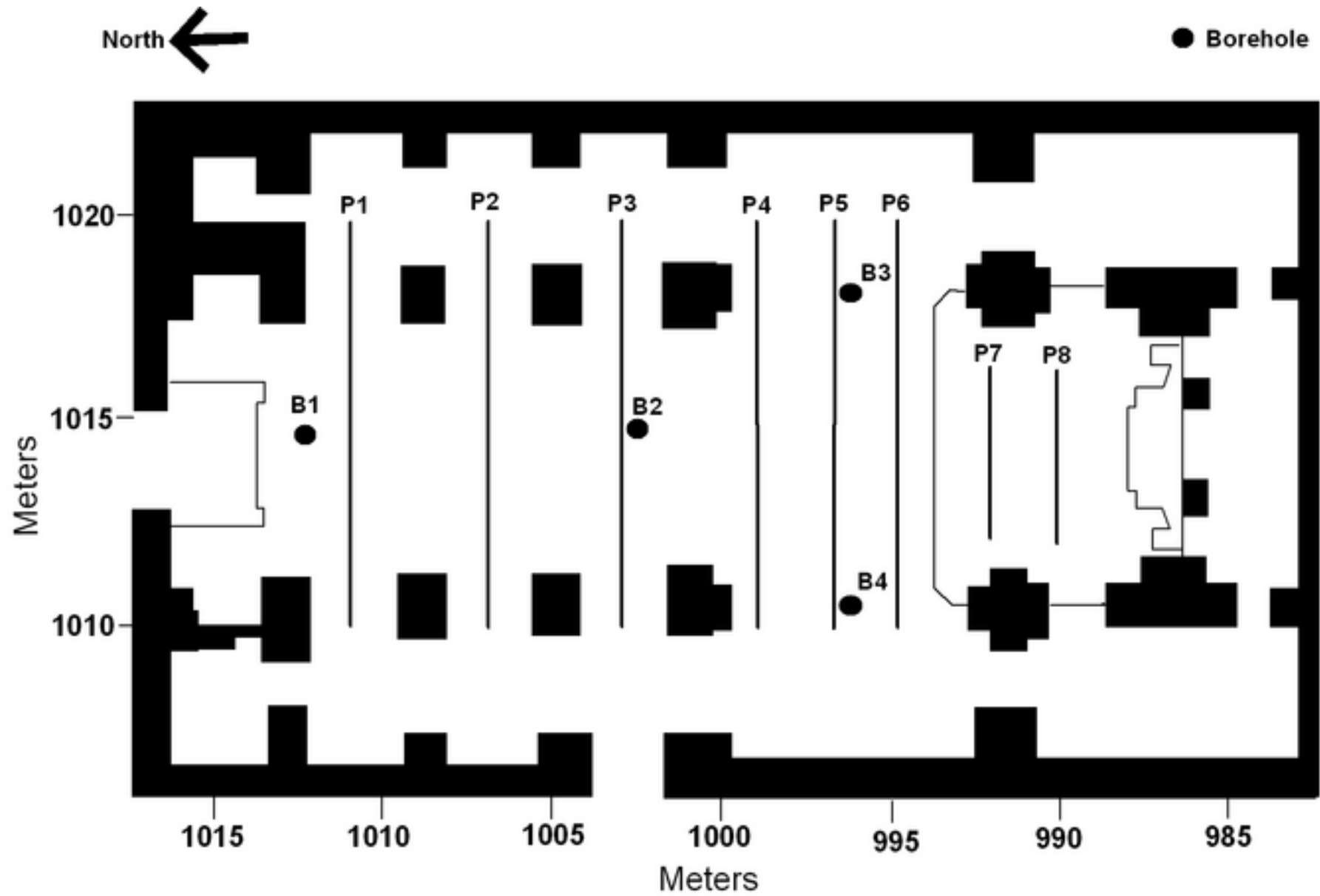


Figure 3
[Click here to download high resolution image](#)

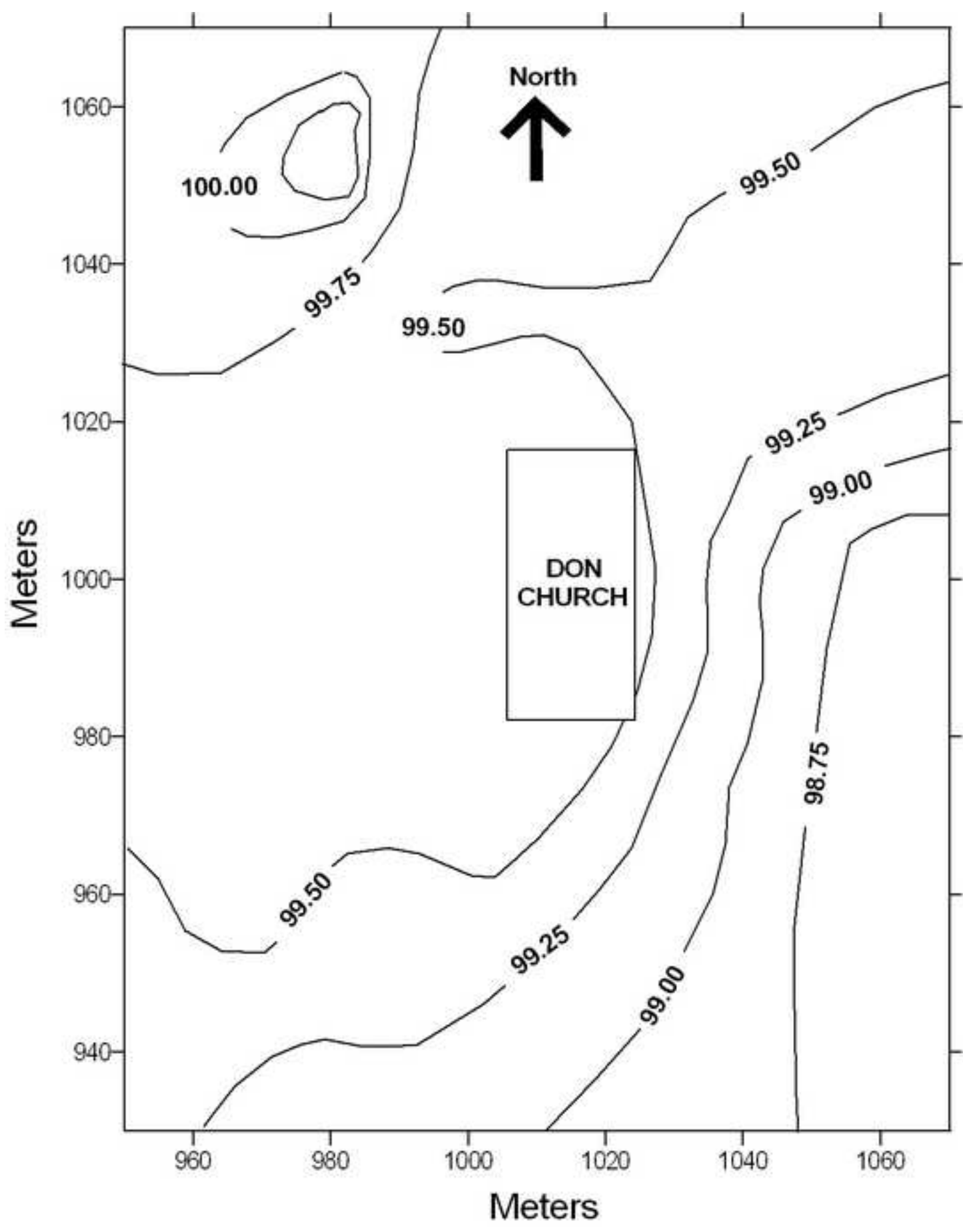


Figure 4
[Click here to download high resolution image](#)

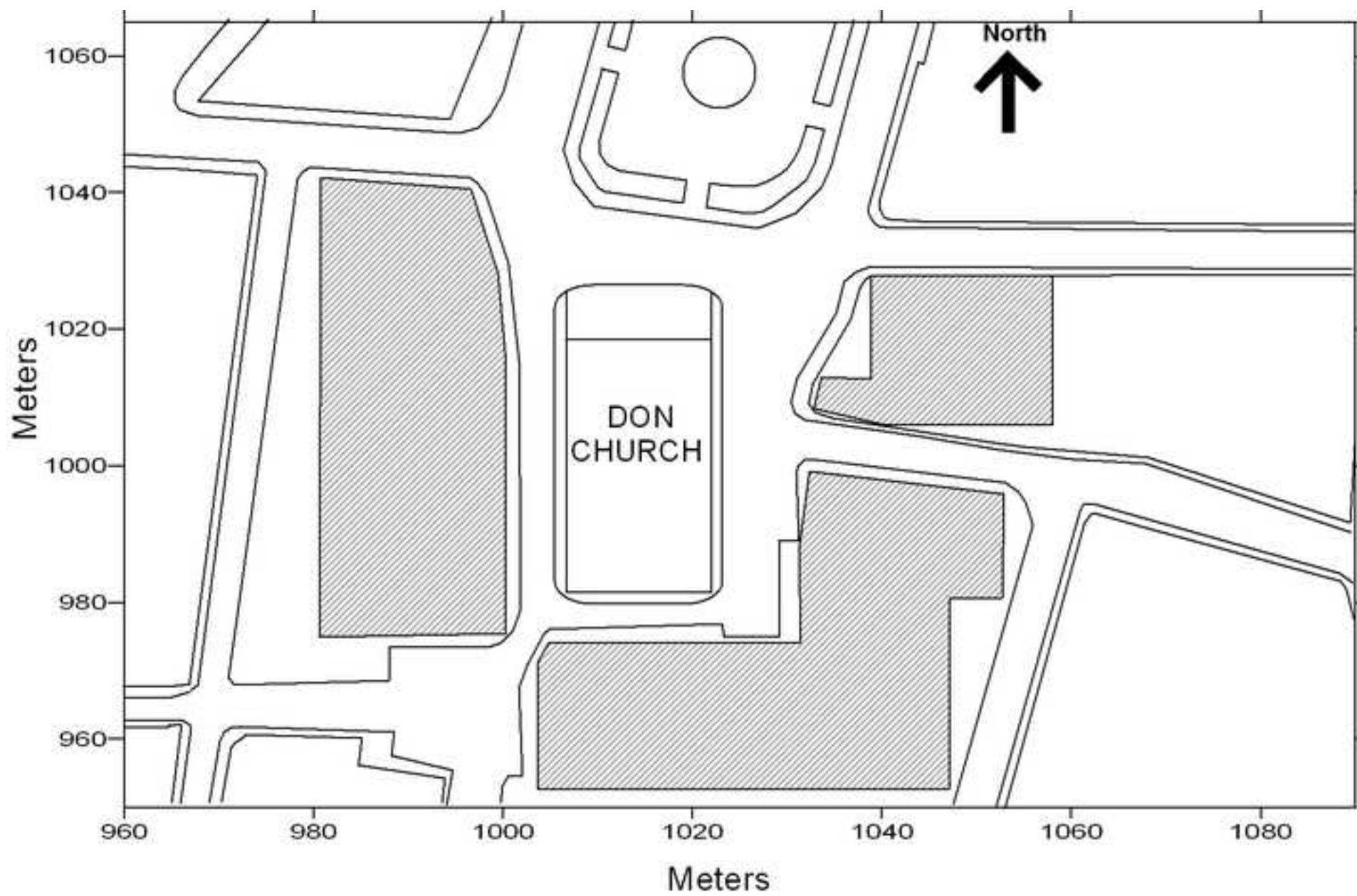


Figure 5
[Click here to download high resolution image](#)

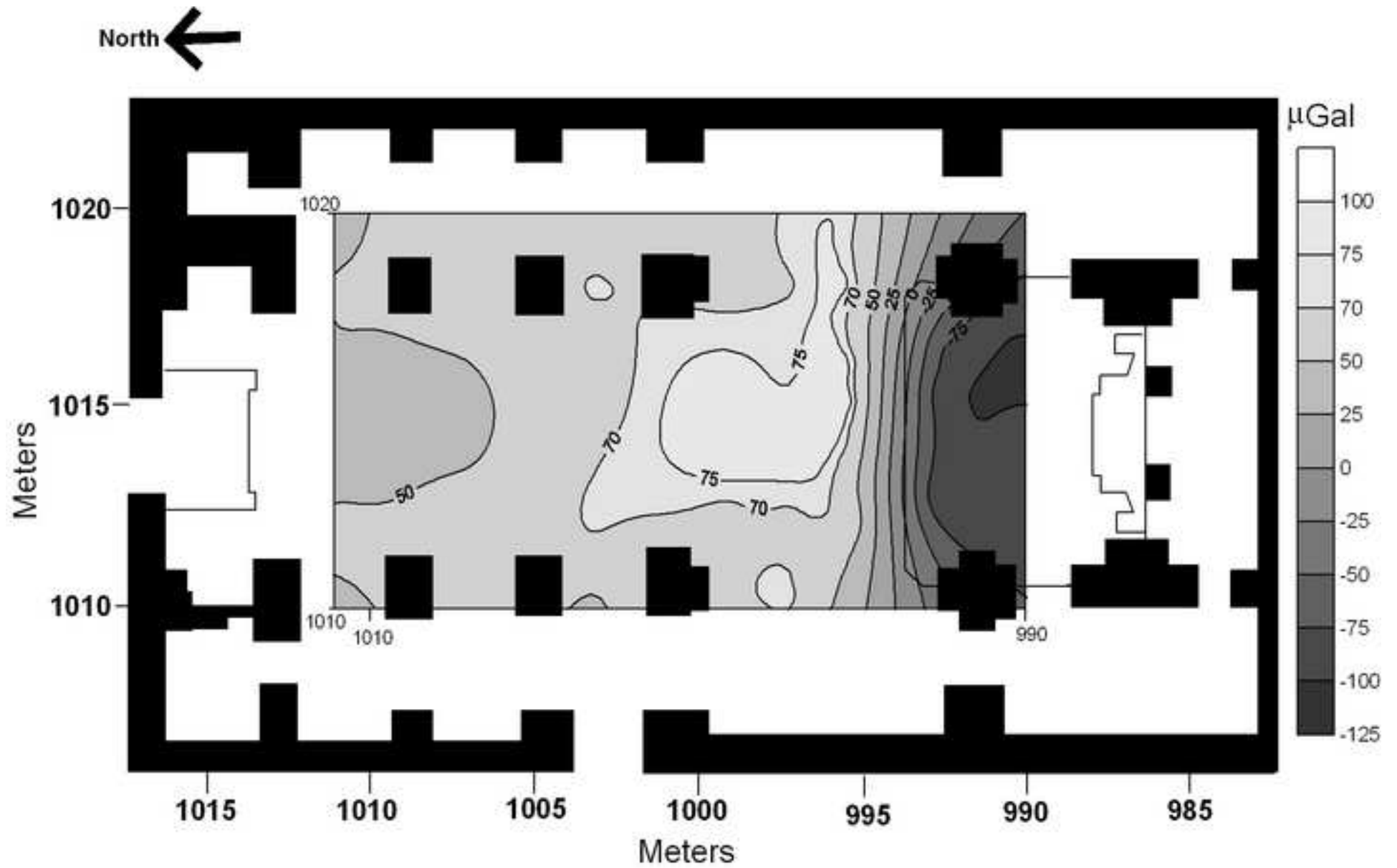


Figure 6
[Click here to download high resolution image](#)

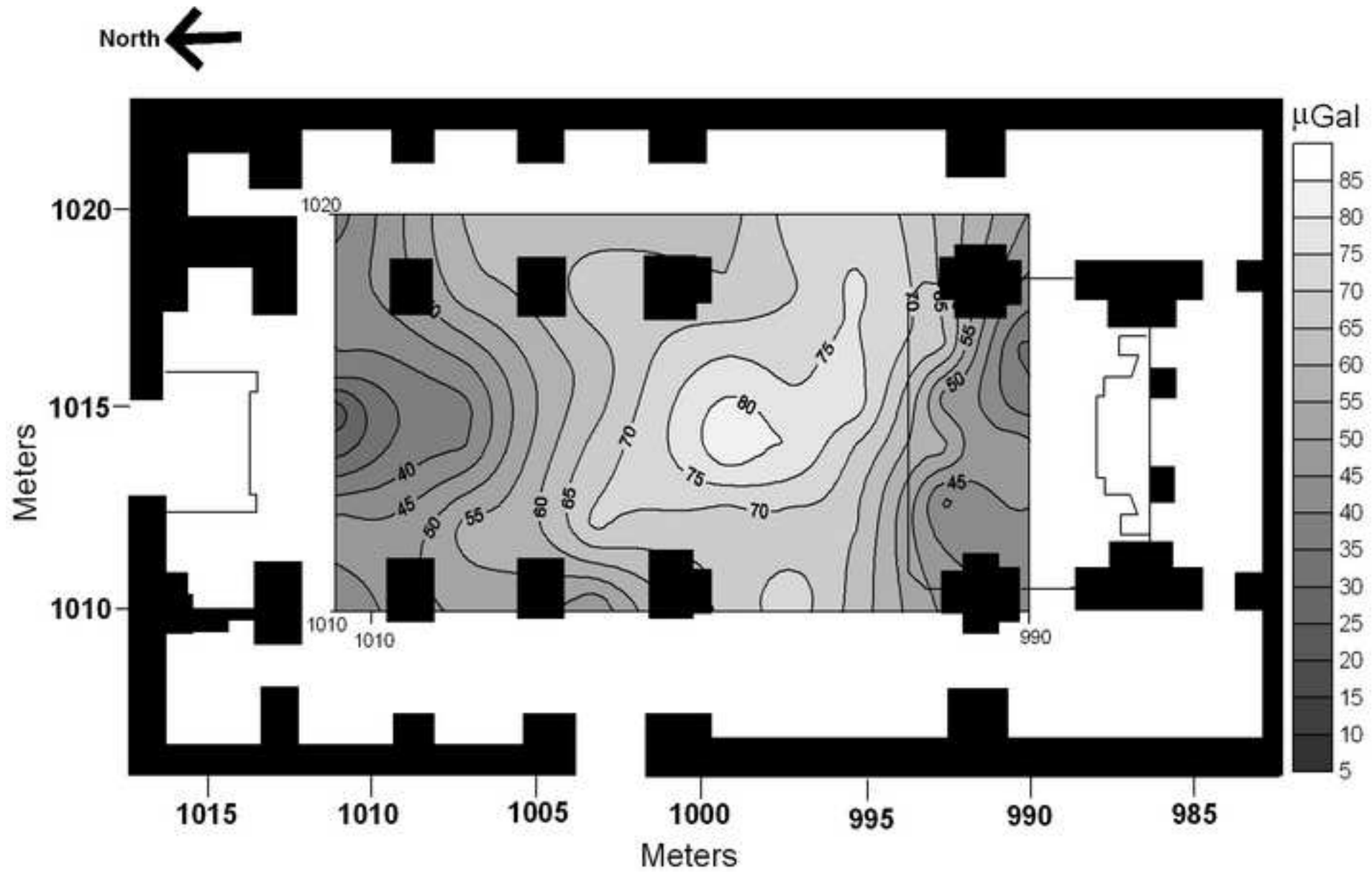


Figure 7
[Click here to download high resolution image](#)

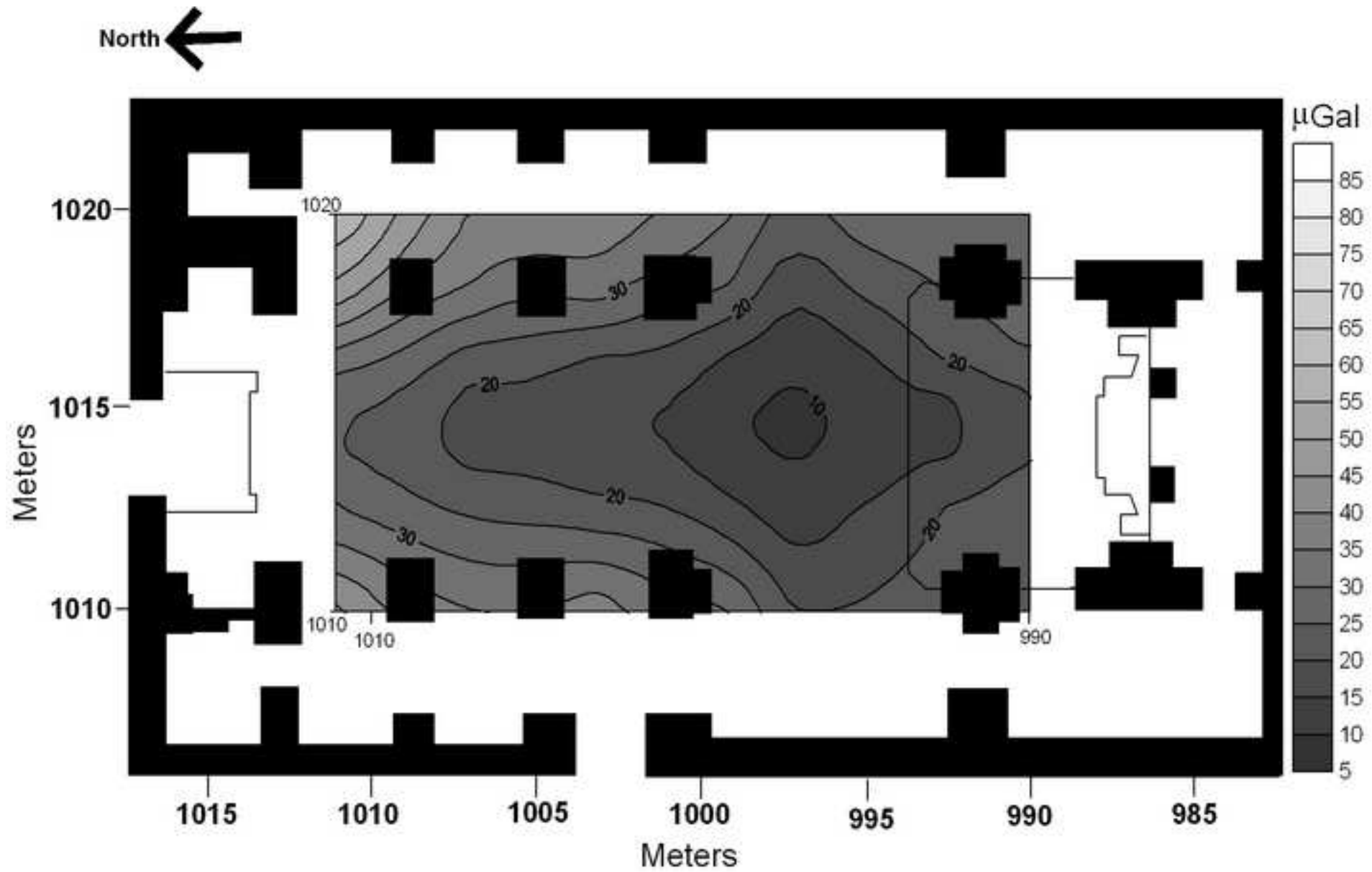


Figure 9
[Click here to download high resolution image](#)

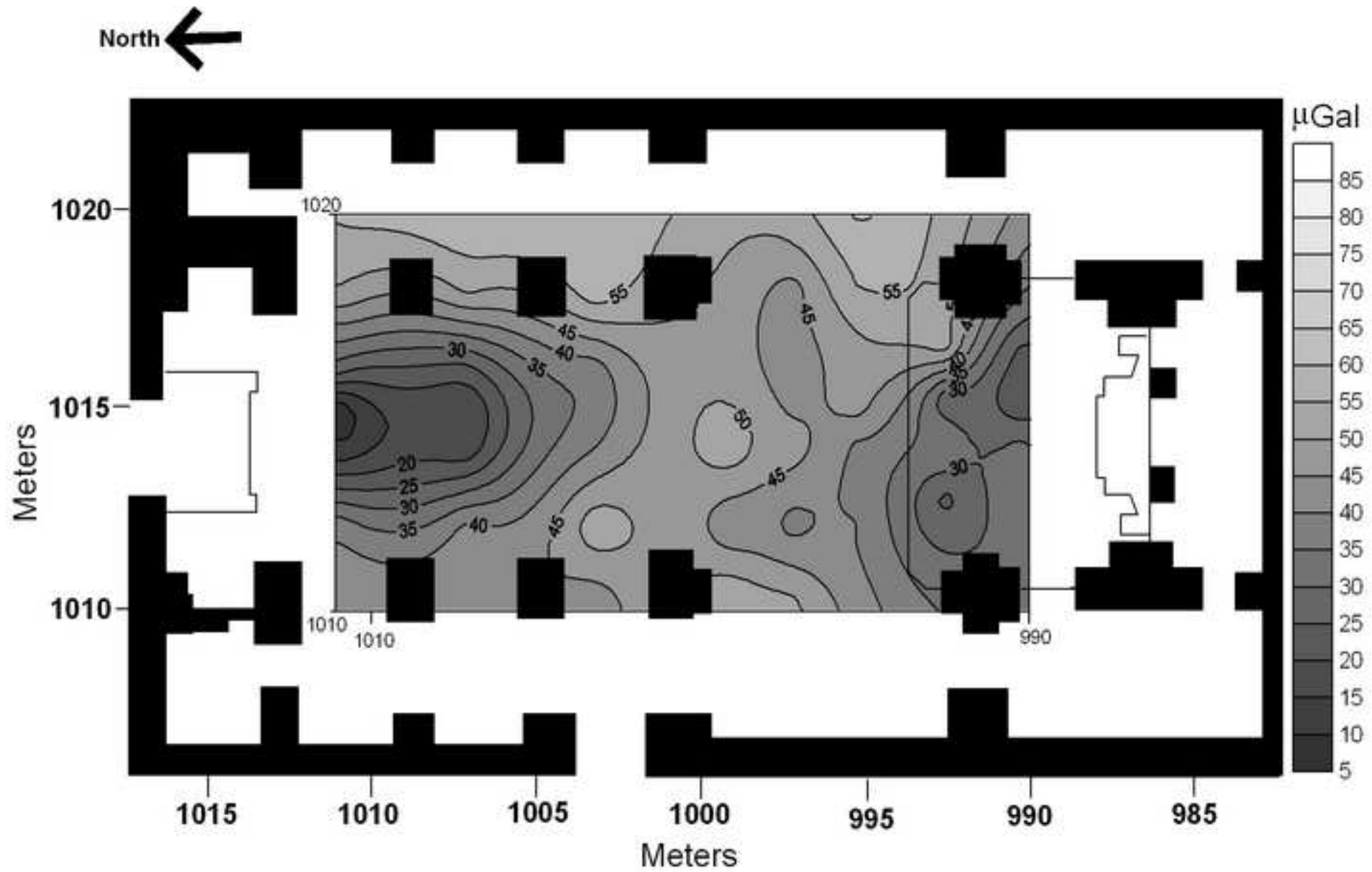


Figure 10
[Click here to download high resolution image](#)

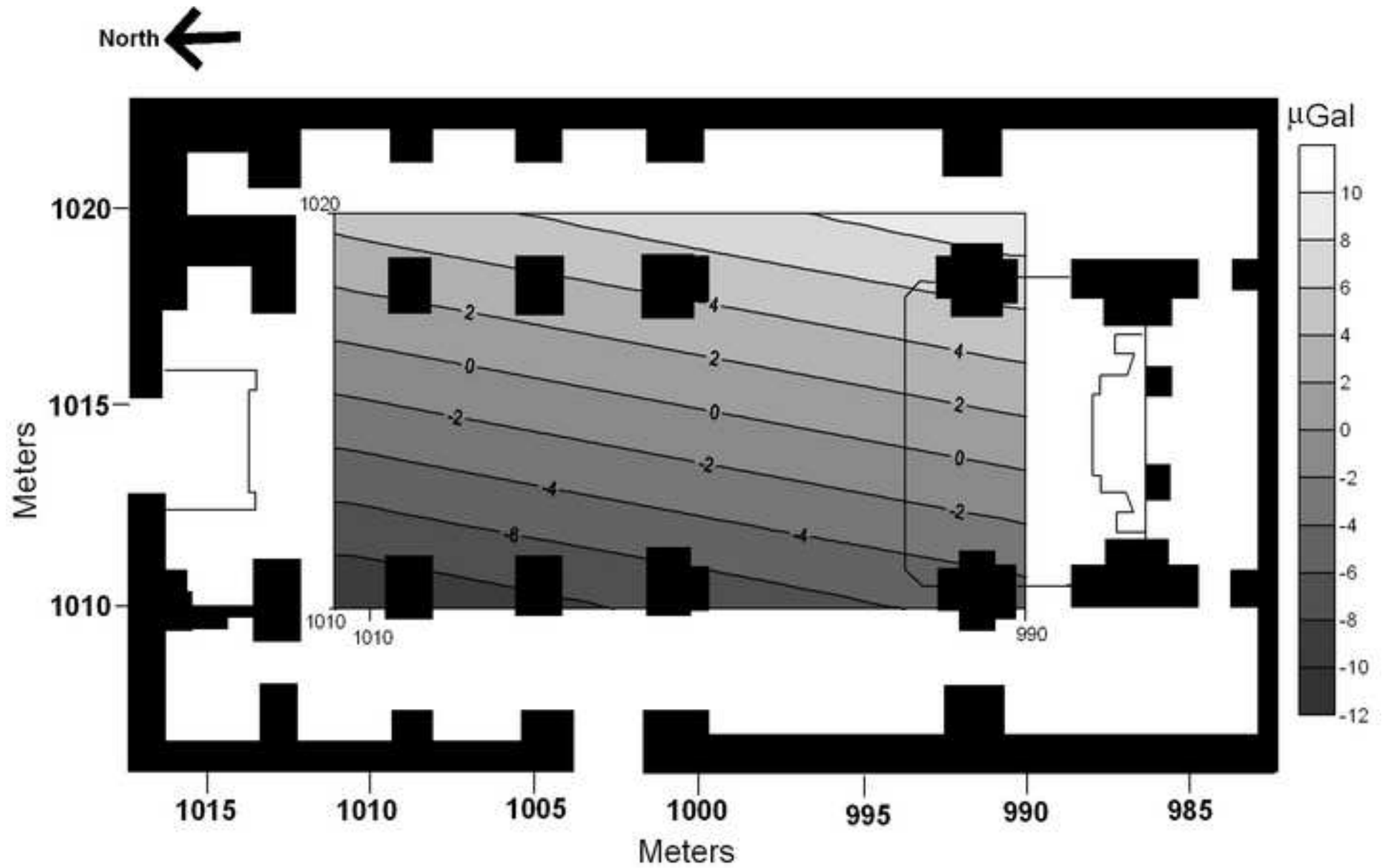


Figure 11
[Click here to download high resolution image](#)

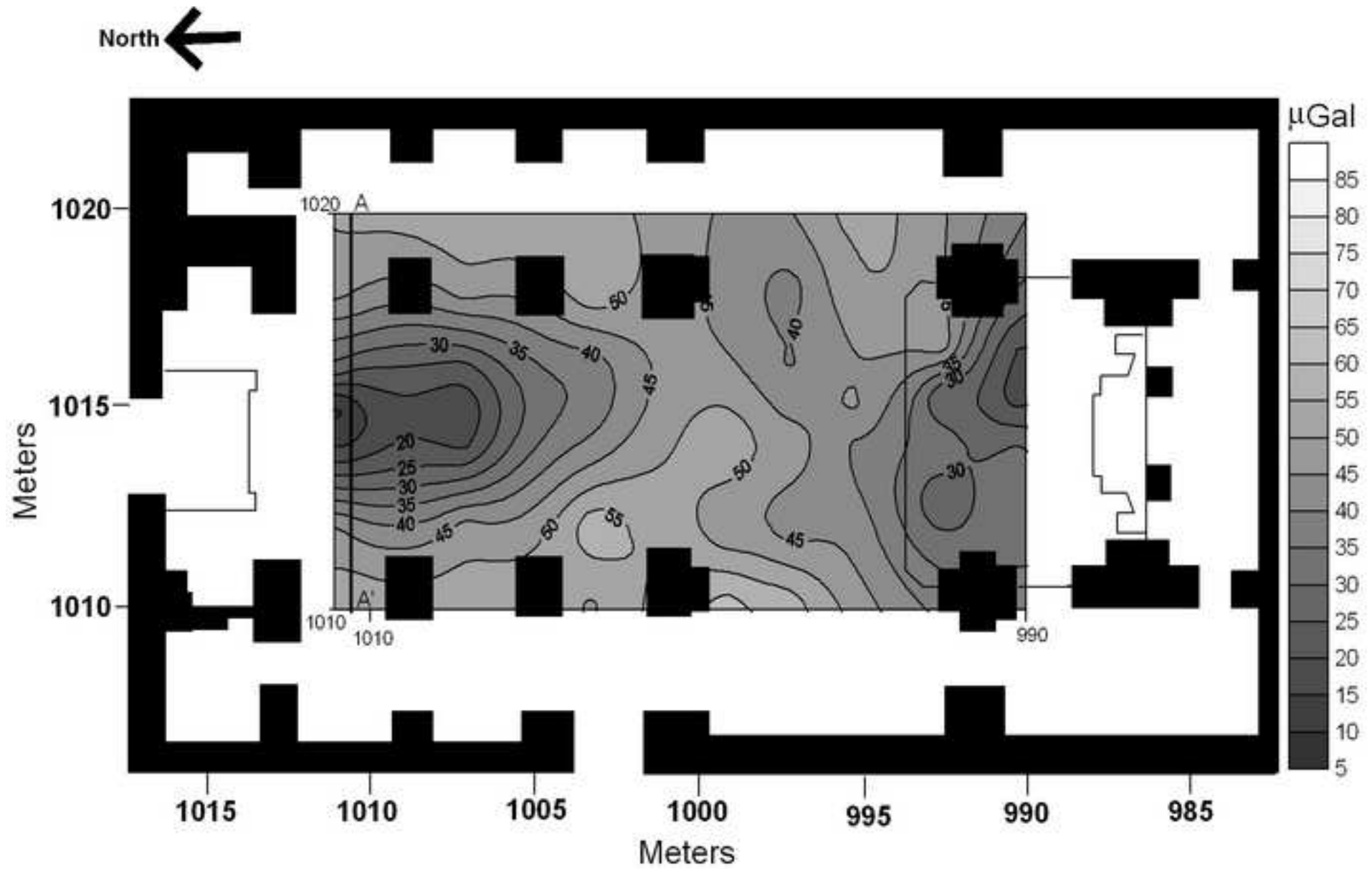


Figure 12

[Click here to download high resolution image](#)

